Effervescent atomization of extra-light fuel-oil: Experiment and statistical evaluation of spray characteristics

J. Broukal[1,*], J. Hájek[1] and J. Jedelský[2]
[1]Institute of Process and Environmental Engineering
[2]Institute of Power Engineering
Brno University of Technology
Technická 2, 616 69 Brno, Czech Republic

Abstract

This paper presents an experimental and statistical analysis of an effervescent atomizer. The spray data were obtained from experimental measurements by means of a Dantec phase/Doppler particle analyzer (P/DPA) and analytical and statistical analysis was performed using MATLAB software. The main goal of this work was to analyze the spray characteristics and to find analytical functions that would fit the experimentally obtained drop size distributions. The fitted distributions were then discretized for modelling purposes and the modelled spray was verified against the experimental data. The discrete spray characteristics will be later used for combustion modelling.

Introduction

Liquid sprays can be generated by various atomizers. For combustion purposes, as in this case, effervescent atomizers are gaining on popularity. The effervescent atomizer is a twin-fluid atomizer with internal mixing, which means that besides the liquid there is one more fluid, typically air, that mixes with the liquid before leaving the atomizer body. This type of atomizer was first introduced by Lefebvre and his colleagues in the late 1980s [1]. Unlike other twin-fluid atomizers, which usually use the air stream to shatter the liquid, the mechanism of drop formation in the case of the effervescent atomizer is rapid air bubble expansion at the atomizer nozzle due to pressure drop. This mechanism makes it possible to use lower injection pressures and larger exit orifice diameters without compromising the drop distribution and has many advantages compared to conventional atomizers [2].

In general, the atomization process is divided into primary and secondary break-up. The primary breakup occurs when the fluid flow exits the orifice and besides being dependent on properties of the fluids involved, it is also strongly dependent on the atomizer type, inner structure and geometry. Secondary atomization is a process during which droplets further break up or collide leading to various outcomes (reflection, coalescence, breakup, etc.). Unlike primary atomization, secondary atomization depends only on properties of the atomized liquid (viscosity, velocity, temperature, surface tension, density, etc.) and the surrounding fluid (typically air).

Recently, several studies appeared (e.g. [3], [4] and [5]), where the atomization process is modelled directly, meaning that both the internal and external flows are resolved using a single approach, typically the Euler-Euler approach, where the atomized liquid and surrounding air are treated as two continuous impenetrable continua. However, this approach has little applicability in practical applications and although such computational models are emerging, they are not viable in most applications due to extreme computational requirements.

Another approach that is less computationally demanding and therefore acceptable for industrial combustion applications is the Euler-Lagrange approach. In this case the gas phase is modelled as a continuum but the liquid phase is treated as a system of discrete particles (droplets) that are tracked in the gas flow field. It is therefore necessary to use appropriate models for primary and secondary breakup (to determine initial droplet parameters like diameter, velocity and direction) as well as for all other processes concerning the droplets like momentum, heat and mass transfer (evaporation). This is the approach adopted in the present work.

This work concentrates on empirical modelling and numerical representation of the primary break-up process. A strongly simplified approach is to work with only a few representative parameters (e.g. Sauter mean diameter, mass median diameter), but if one wishes to represent the spray more precisely it is necessary to characterize the entire drop size distribution. This method has been developed and studied in numerous papers. Sovani et al. [2] and Jedelský et al. [6] suggest that Rosin-Rammler distribution is appropriate for effervescent atomizers. The Rosin-Rammler distribution function reads

$$Q = 1 - e^{-(D/X)^q},$$

* Corresponding author: broukal@upei.fme.vutbr.cz

where D is the drop diameter and Q represents the mass of drops whose diameter is smaller than D. The parameter X corresponds to the drop diameter for which 63.2 % of the drops' mass is smaller, while the parameter q is a measure of uniformity of the diameters [7].

Moreover, Jedelský et al. also uses log-normal distribution to fit the experimental data. Calay and Holdo [8] and Cleary et al [9] use the two above mentioned distributions to model flashing jets. Ayres et al. [10] presents a more theoretical approach by predicting joint distribution for both size and velocity of the droplets in sprays using the maximum entropy formalism. A comprehensive list of drop size distributions can be found in [11].

Modern CFD software codes often allow users to choose from predefined atomizer models and thus avoid laborious manual setting of the spray injection. These models (mostly empirical) use physical atomizer parameters to calculate initial drop sizes, velocities and positions. In the case of Ansys Fluent, a model for the present effervescent atomizer is not available and therefore it is necessary to use a simpler approach (for example cone injection) and to set it up carefully to obtain the spray characteristics as required. Although a great deal of research has been made in CFD modelling of internal combustion engines [12,13] many papers deal with CFD modelling and numerical studies of non-combustive sprays. Xiong et al. [14] performed a three-dimensional simulation of an effervescent atomizer. They developed a model for primary and secondary break-up based on the model of Lund et al. [15]. Qian et al. [16] continued in the footsteps of Xiong et al. and developed a model for effervescent atomizers with an impinging plate. Calay and Holdo [8] used CFD tools to predict dispersion of flashing jets and a review of physical models and advanced methods used in CFD of sprays can be found in [4].

The scope of this work is to develop a software for analysis of the experimental data and to verify the Fluent ability to represent effervescent sprays. The software will be used firstly to analyze the raw data obtained from measurement and also to find the best possible analytical fit. The fitted data will be discretized and used as input for the CFD software Ansys Fluent, where spray simulations will be performed. Simple models will be preferred in order to focus on the injection models. Finally, the computed data will be compared with the experiment and the results will be discussed.

Measurement and Data Processing

The measured spray of extra-light fuel-oil was generated using the effervescent atomizer and operating conditions described in [17] as configuration E38. Drop sizes and drop velocities were measured using a Dantec phase/Doppler particle analyzer (P/DPA) in 6 radially equidistant sampling points at 150 mm from the atomizer orifice. The angle depicted in Figure 1 represented the spray half-angle and was estimated as the angle between the axis and the farthermost measurement point. A detailed description of the measurement can be found in [17].

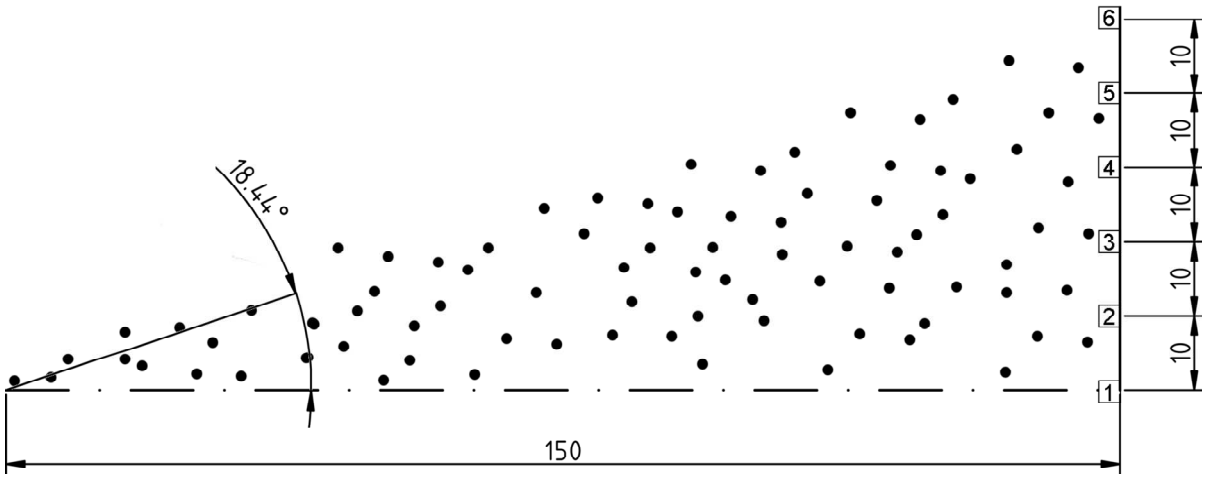

Figure 1. Schematics of the spray measurement

For the purpose of data analysis a software with graphical user interface using MATLAB programming environment (see Figure 2) has been created. The software is able to load experimental data from multiple measuring points as generated by the measuring device and to display frequency and mass histograms together with representative diameters (SMD, MMD, D10, D20, etc.). For simplicity it was assumed that spray properties are piecewise constant in the radial direction, i.e. that a parameter measured in a certain sampling point is the same for the annular area with radiuses $x+d/2$ and $x-d/2$, where r is the radial distance of the sampling point and d is the distance between two adjacent sampling points. The user can then choose from a variety of analytical functions to fit the experimental data. So far the following distributions were implemented: log-normal, root-normal, upper-limit, Rayleigh, Rosin-Rammler, Nukiyama-Tanasawa, Beta and Gamma. To calculate the

empirical parameters, the software uses the Nelder-Mead simplex algorithm [18], in order to accommodate nonlinear regression.

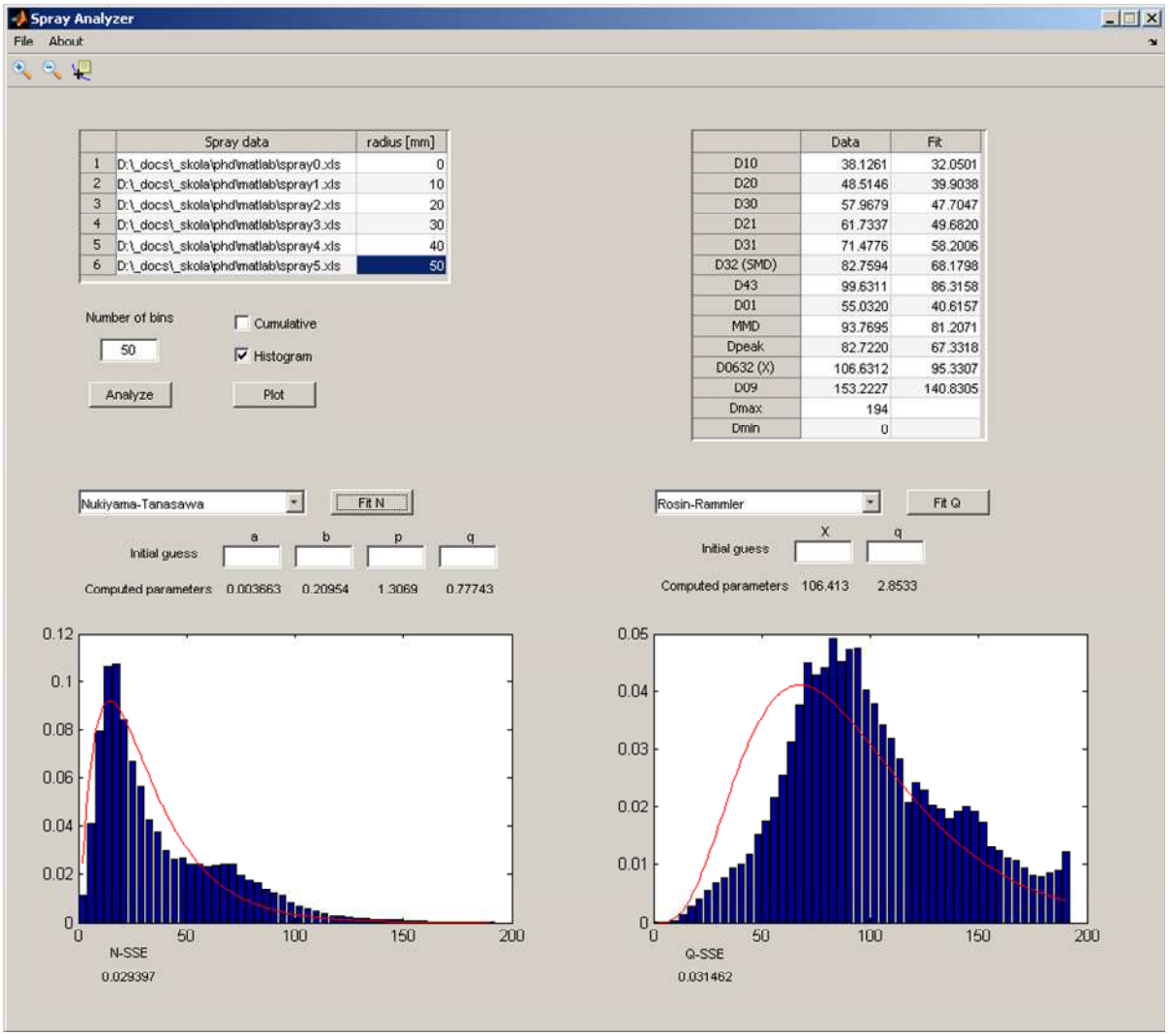

Figure 2. Overview of the developed software

Two cases were studied in this paper. In the first case (A) the spray was considered as a whole and the best Rosin-Rammler fit was found. In the second case (B) the data from the first four sampling points (starting from the centreline) were analyzed separately as well as the two remaining sampling points. This separation was performed due to large qualitative differences observed in the three datasets. Best Rosin-Rammler fits have been found for each of these three datasets. Despite of not giving the best approximations the Rosin-Rammler distribution was used in the fitting procedure due to the fact, that Ansys Fluent (used for flow modelling in this work) is equipped with a pre-prepared procedure to discretize this particular distribution function. The best fit in terms of number distribution was the log-normal distribution and in terms of mass weighted distribution the root-normal distribution.

A similar discrepancy, as seen in the work of Babinski and Sojka [11], has been found between measured and calculated mass flow rates of the atomized liquid. The calculated mass flow rate did not agree with the measured one and therefore needed to be corrected. Such behaviour is probably caused by the low accuracy and error rate of the measurement technique.

Measurement results

The drop size distributions (notably frequency distributions) in several of the sampling points in the measured spray were bimodal. The distributions obtained from the measurement points close to the atomizer centreline exhibited unimodal behaviour, but bimodality manifested itself as the distance from the centreline

increased (see Figure 3). The overall frequency distribution is slightly bimodal (the second peak is around 70 μm).

The mass distributions for respective measurement points on the other hand do not display bimodality, but they generally exhibit discontinuities in the large drop size end of the distribution. These discontinuities might be caused most probably by the measuring technique.

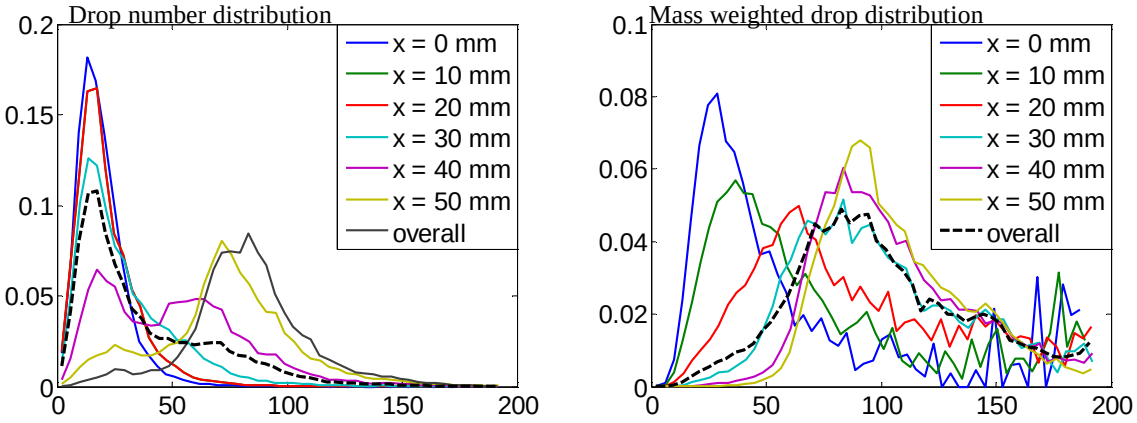

Figure 3. Frequency and mass distributions at different measurement points and average overall distributions, x represents the radial distance of the measurement point

Modelling

The goal of the modelling part of this work was to verify the ability of commercial Ansys Fluent software to re-create a spray according to experimental measurements. This naturally does not mean only the possibility to create suitable boundary conditions, which is a matter of course. The goal was rather to perform a computational virtual experiment repeating the original measurements in which data on the spray were collected. The subjects of evaluation thus include the way how spray boundary conditions are set up, how droplet motion is simulated and how the interaction of the droplets with air deforms the spray on its way from nozzle orifice to the measuring location.

A three-dimensional cylinder-shaped domain was created in Gambit software. The diameter of the domain is 400 mm and it is 2200 mm long. The mesh consists of nearly 80000 hexahedral cells. The domain was filled with air and the spray originated on the centreline 200 mm from air inlet base of the cylinder. The spray was injected from a small circular area of diameter 2.5 mm representing the actual nozzle orifice. In the position of measuring location 150 mm downstream from the injection a series of concentric annular control surfaces has been set up that enabled the virtual measurement. This model served as a test stand for evaluation of the capabilities of the flow solver.

In order to keep the model as simple as possible, gravity was neglected. Turbulence has been accounted for by the $k - \varepsilon$ realizable turbulence model with the default settings [19]. The spray itself has been modelled as a set of Lagrangian entities using the Discrete Phase Model (DPM). Ansys Fluent offers a variety of atomizer models and injections. Unfortunately none of the implemented atomizer models does correspond to the specific measured effervescent spray; therefore it was chosen to use cone injections instead. In the case A only one injection was created to represent the whole spray, namely a so-called solid cone injection, which means that the spray with a specified half-angle is at the orifice homogeneous with respect to drop size. In case B one solid cone injection and two hollow cone injections were created. The Rosin-Rammler distribution parameters for each injection where found using the previously described MATLAB code. It was also necessary to input the minimal and maximal drop diameter and number of diameters (N) included in the simulations. Each of the drop sizes is in the simulation represented by a specified number of particle streams. Fluent then chooses N diameters equidistantly from between the minimal and maximal diameter and computes for them the Rosin-Rammler probability density using the specified empirical PDF. Then to each stream a different mass flow rate is assigned depending on the computed value of the PDF.

A separate computational analysis was performed to determine the minimal amount of particles that can realistically represent a spray. The criterion used for the evaluation was of the symmetry of temperature distribution in a simple spray combustion problem. The numerical configuration described above is the result of this assessment. The simulations were carried out on the same grid and with the same inlet conditions as in cases A and B. The combustion model was based on a single-step global chemistry with reaction rate controlled by

turbulent mixing (so-called eddy dissipation model). Radiative heat transfer has been included using discrete ordinates method to obtain more realistic temperature field. Cases with 500, 2000, 4000, 6000, 8000 and 12000 particles were tested by qualitative comparison of temperature contour plots (see Figure 4). The smallest number of particles using which the temperature field was still appropriate was found to be 6000.

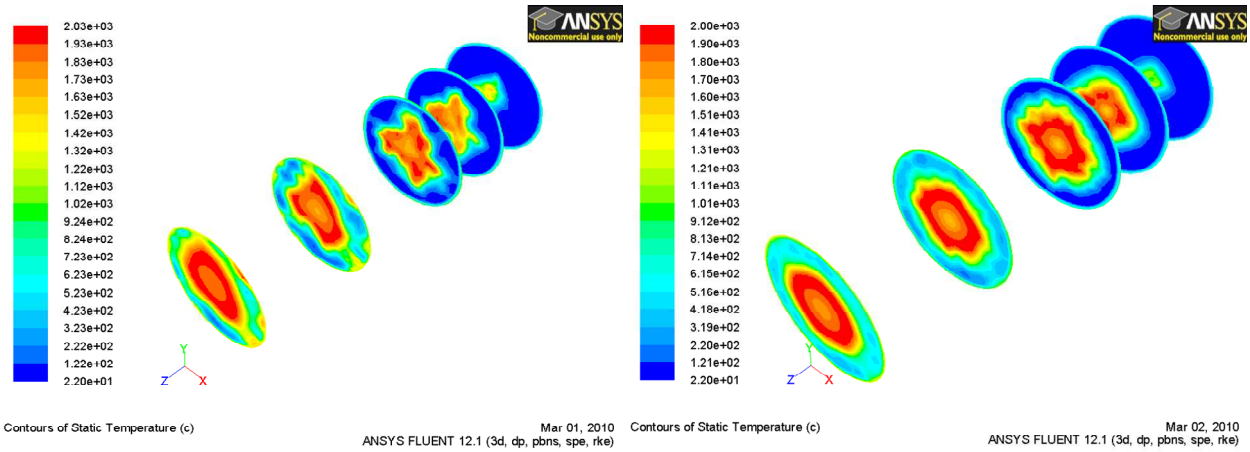

Figure 4. Illustrative demonstration of temperature contour plots. The contours are displayed on cuts perpendicular to the spray axis at 200, 300, 400, 700 and 1100 mm from the spray origin. On the left there are 500 particles while the picture on the right has 6000 particles

The total number of streams both in the case of a single injection (case A) and in the case of three injections (case B) was 200. In the latter case this number has been divided among the injections depending on the area ratios represented by corresponding measurement points. Together with 30 discreet diameters per stream it gives 6000 computational particles.

Another input in the injection definition is the discharge velocity, which was approximated using a formula derived by Jedelský and Sláma in Appendix 2 of [17]. In the case B it was necessary to divide properly the mass flow rates of the three injections. This was done by analyzing the partial mass flow rates in respective sampling points and relating them to the total mass flow rate. See Table 1 for injection parameters of the cases A and B.

Although flow in the problem was treated as steady, Ansys Fluent enables to track the particles either as steady (Steady Tracking – StTr) or unsteady (Unsteady Tracking – UnTr). To predict the particle trajectory, one has to integrate the force-balance equation, which can be written (for the *x* direction in Cartesian coordinates) as follows:

$$\frac{du_p}{dt} = F_D\left(u - u_p\right) + \frac{g_x\left(\rho_p - \rho\right)}{\rho_p} + F_x\,, \tag{1}$$

where u_p is the particle velocity, u the surrounding air flow velocity, F_x and g_x is an additional acceleration in x direction and gravity respectively. $F_D(u - u_p)$ is the drag force per unit particle mass [19]. The shape of drops is assumed to be spherical and the drag force was calculated using the formula that reads

$$F_D = \frac{18\mu}{\rho_p d^2}\frac{C_D\,\mathrm{Re}}{24}\,, \tag{2}$$

where d is drop diameter, μ is the molecular viscosity of the fluid (air) and

$$C_D = a_1 + \frac{a_2}{\mathrm{Re}} + \frac{a_3}{\mathrm{Re}^2}\,. \tag{3}$$

The constants a_1, a_2, a_3 apply to smooth spherical particles over several ranges of Re given by Morsi and Alexander [20]. Ansys Fluent numerically solves the integral by choosing a time step which can be defined using the so called step length factor (SLF). It allows Fluent to compute the time step size in terms of the number of time steps required for a particle to traverse a computational cell [19]:

$$\Delta t = \frac{\Delta t^*}{SLF}, \quad (4)$$

where Δt^* is the estimated transit time. All units in the previous equations are SI units. In this study two different SLF have been tested: 5 and 15.

In order to take into account the turbulent flow effects on particle motion, the Discrete Random Walk (DRW) model has been applied. The DRW model simulates the interaction of a particle with a succession of discrete stylized fluid phase turbulent eddies.

The discrete phase exchanges only momentum with the continuous phase. Mass and energy exchange (due to evaporation) has been neglected as the analyzed cases did not include combustion and the ambient temperature was around 20°C. For such conditions the region of interest is sufficiently small, so that the diameter of drops does not change considerably before reaching the sampling plane. Due to the nature of the studied prob-

lem, where we want to model a spray using experimental data at 150 mm from the atomizer orifice, secondary atomization (drop collisions, break-up and coalescence) has not been included.

Sampling in the computational spray was performed by a user-defined function (UDF), which monitored drop parameters at annuluses corresponding to each measuring point 150 mm from the spray origin. After a particle travels further than 250 mm from the spray origin it is deleted in order to decrease computational costs.

In the simulation a small air co-flow (1 m/s) was introduced. The co-flow was used in order to improve solution stability. On the opposite side of the domain was used pressure outlet condition. The cylinder's lateral surface was treated as a wall with no slip conditions. This boundary condition deviates from the experiment, but since the volume of interest is relatively small in comparison with the domain dimensions, it should not affect the solution significantly.

Convergence of the simulation was proclaimed upon stabilization of instantaneous flow velocities in various points and total mass of fuel-oil in the computational domain.

Table 1. Injection parameters for cases A and B

	Case A	Case B		
Injection type	Solid cone	Solid cone	Hollow cone	Hollow cone
Half-angle [deg]	18.44	11.31	14.93	18.44
Mass flow [g/s]	21.8	11.3	6	4.5
X[μm]	106.4	103.5	106.7	107.5
q	2.85	2.29	3.56	3.94
measuring points included	1-6	1-4	5	6
# of streams	200	81	53	66
# of diameters (*N*)	30			
Discharge velocity [m/s]	156.72			
Fuel-oil density [kg/m^3]	874			

Results and Discussion

Discussion of Case A

In this case the whole spray was substituted by a single solid-cone injection. Different cases were studied depending on the tracking scheme and step length factor. The results showed that there is almost no difference between the two values of step length factor (SLF = 5 and SLF = 15) both in the partial and in the overall drop distributions. Such small significance of the SLF is probably induced by the simplicity of the model. In the case of a stronger coupling between the phases (mass and energy exchange, combustion) the significance of SLF would probably increase. Nonetheless future investigation in the area of SLF significance is needed.

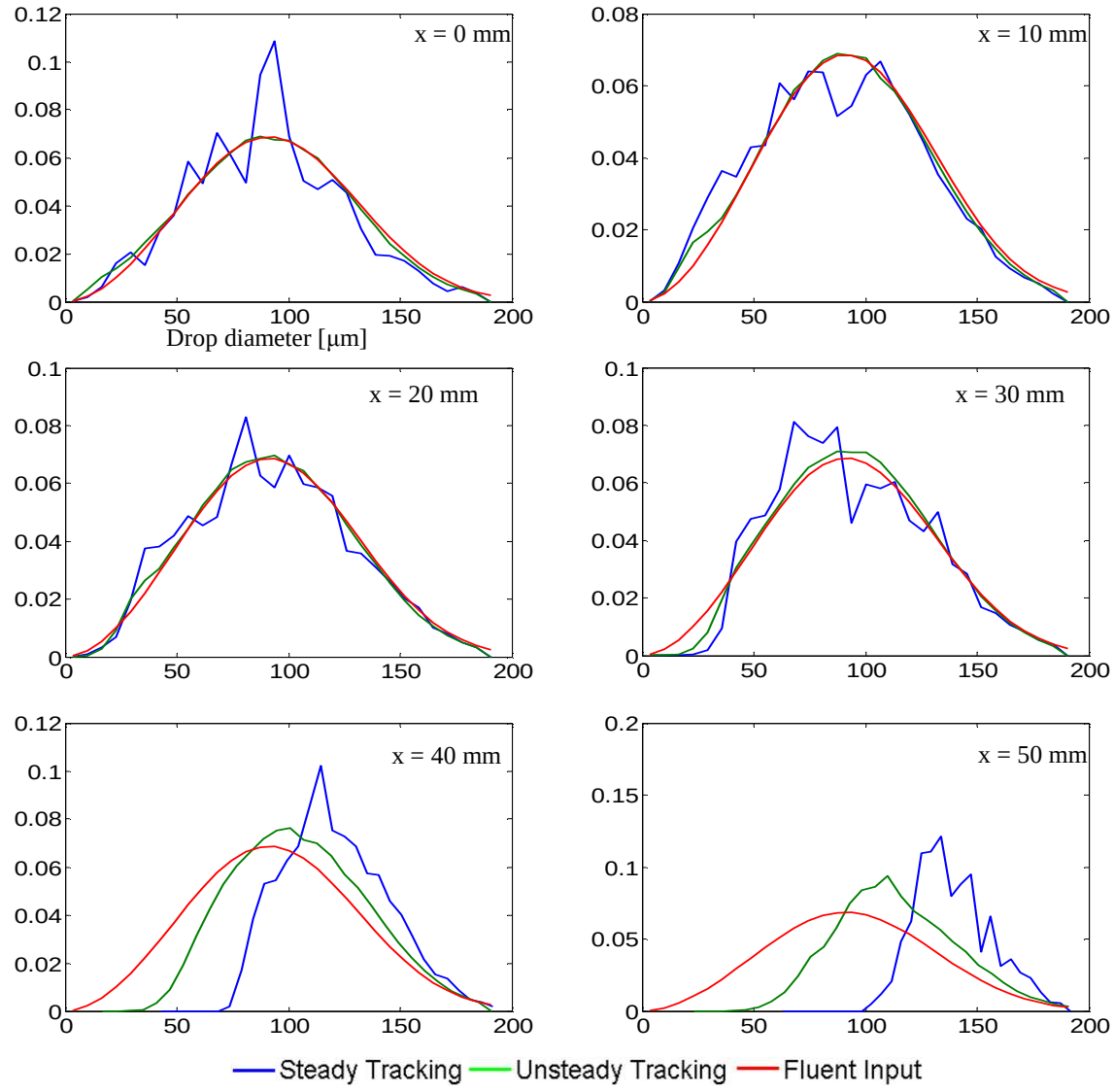

Figure 5. Comparison of steady and unsteady tracking results in case A

On the other hand the tracking scheme has a remarkable effect on the drop distributions. From Figure 5 it is clear that the unsteady tracking scheme gives superior results when compared to steady tracking. Despite the fluctuations of the steady tracking scheme both results are close to the input drop distribution up to the fourth measurement point (at x = 30 mm). In the last two measurement points the calculated distributions differ from the input distribution; the steady case differs more significantly. This shift is probably caused by the smaller particles being entrained in the spray core. The last two measurement points in Figure 6 show that in the case of unsteady particle tracking, the calculated drop distributions represent surprisingly well the (local) RR fit of actual drop distributions in the respective measurement points. The slight under prediction of smaller diameters

in these last two points might be caused by the absence of secondary atomization, which is responsible for the creation of smaller drops in the peripheral regions.

In Figure 6 it can be also clearly seen that closer to the spray core the input distribution is conserved well, however the Rosin-Rammler fits in the individual measurement points (green curves) differ heavily. This is a clear evidence of high complexity of the drop formation process, which cannot be simply replaced by an overall drop distribution when trying to model the spray accurately.

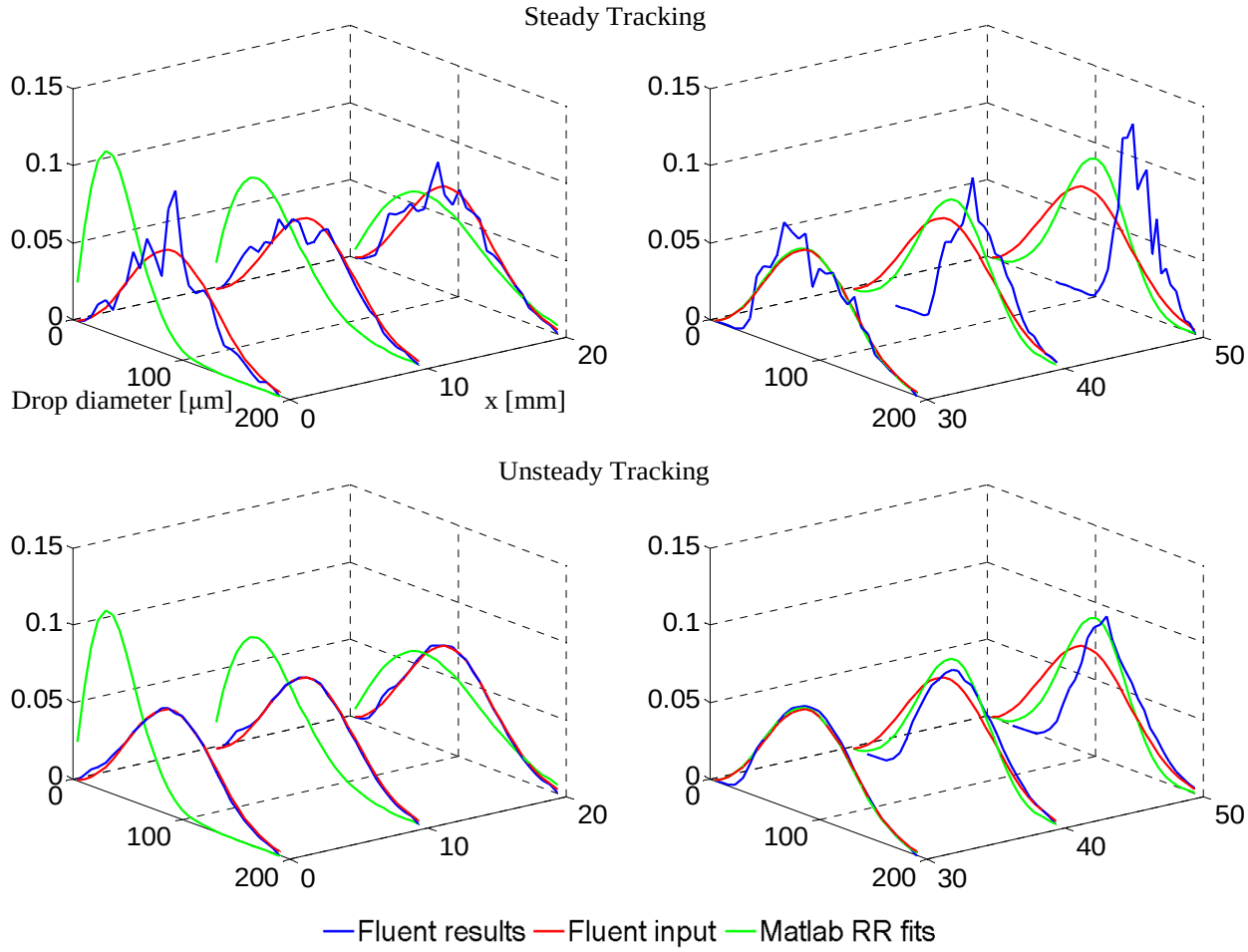

Figure 6. Drop mass PDF for case A, x represents the radial distance of the measurement point

Discussion of Case B

In the second case the whole spray was modelled using one solid cone and two hollow cone injections. The inner solid cone injection averaged the spray cone up to the fourth measuring point (starting from the axis) and each of the two hollow cone injections represented spray sections relative to the last two measurement points. As in the previous case the step length factor did not act as a major deal breaker. Unfortunately the steady tracking results were not examined due to unresolved issues in the user defined function used for numerical spray evaluation. Therefore all results for the case B were produced with the unsteady tracking option. In Figure 7 is evident, that starting from the first measurement point a small peak is building up around the value 70 μm and it reaches its maximum in the fourth measurement point (at x = 30 mm). A possible explanation of this behaviour is a large entrainment of smaller drops at the interface between the inner solid cone injection and middle hollow cone injection due to the coarse spatial angle discretization. It is also not possible to exclude the possibility that the particle tracking model gives unsatisfactory results when dealing with multiple concentric injections. The peak vanishes almost immediately when moving to the spray outer regions.

An interesting observation can be made when comparing the last two measurement points in case A (Figure 6) and case B (Figure 7). In case A the calculated drop distributions are closer to the Rosin-Rammler fits in the individual measurement points than the calculated drop distributions from case B. This might be again caused by the coarse spatial angle discretization.

Similarly to the previous case A (single cone injection) the calculated distributions in the spray core show good preservation of the input distribution (omitting the measurement point x = 30 mm) while in the last two

measurement points a shift is observed. The reason of this shift is identical to the shift discussed in case A. In the measurement points x = 40 mm and x = 50 mm the green curve is missing because in this case it is identical to the red curve.

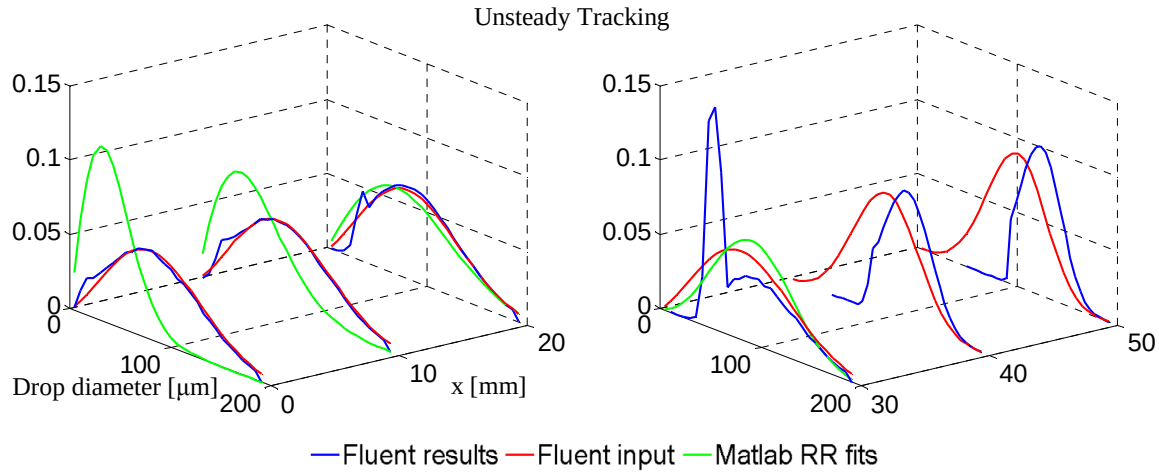

Figure 7. Drop mass PDF for case B, x represents the radial distance of the measurement point

Overall drop distributions of both studied cases can be seen in Figure 8. Concerning the case A, according to Figure 8, it might seem that there is almost no difference between steady and unsteady tracking. However, differences pointed out in previous paragraphs would probably play a much more important role when dealing with more complex flow problems (i.e. spray combustion). A more noticeable difference is found in case B.

In terms of convergence and solution stability the unsteady tracking scheme behaves better than steady tracking scheme in both cases. The obvious drawback of unsteady tracking is higher computational demand, which is in terms of time approximately two to four times higher.

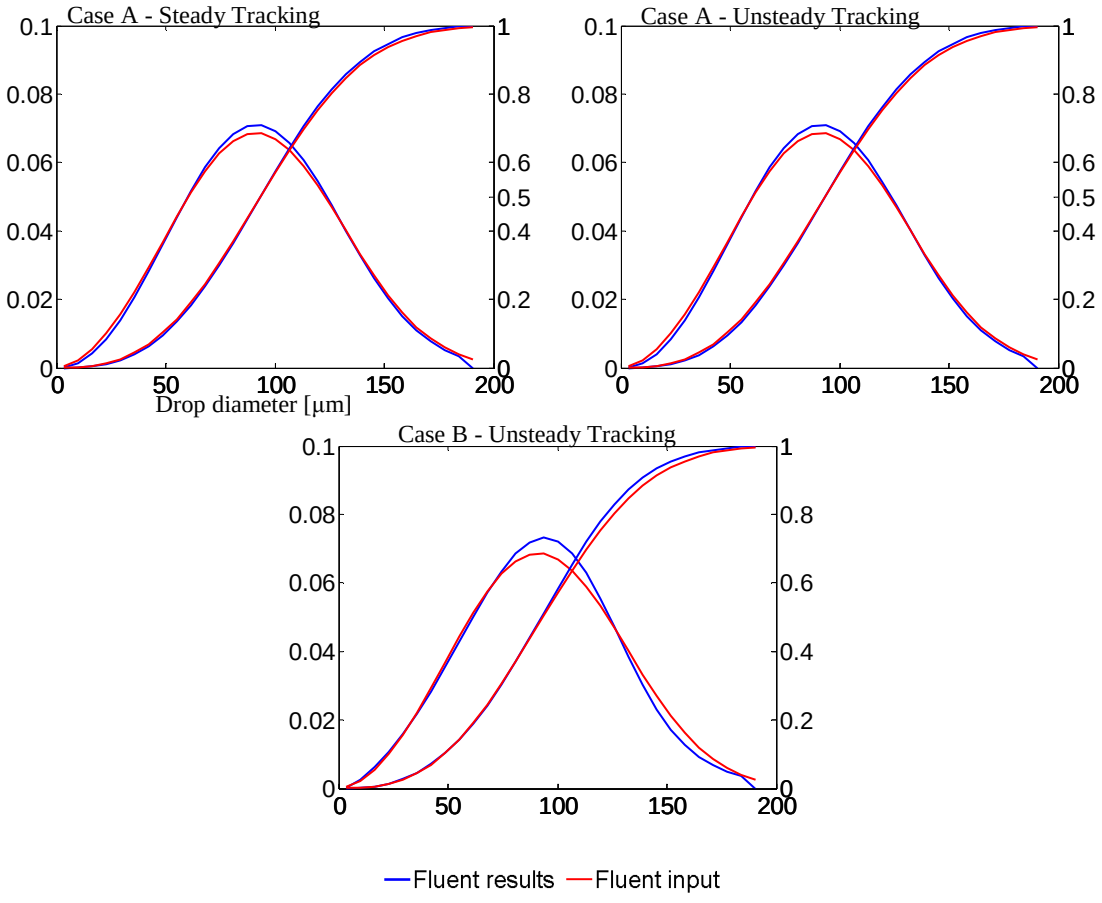

Figure 8. Overall drop mass PDF and distribution functions

Future Work

The software used for the scope of this work offers only basic fitting procedures at the moment. A bimodal approximation, more accurate than the standard unimodal approximations of the effervescent spray, was investigated as a potential improvement, but has yet to be assessed similarly as the two cases reported in this work. In the future research will be employed also other methods, which do not depend solely on experimental results (Maximum Entropy Formalism [11], variations of Lund's model [14], etc.).

The developed spray model will be used to model spray combustion of vegetable oils in large scale combustors. The computed results will be verified in terms of wall heat fluxes with experimental results from a large scale experimental facility [21].

Conclusion

Raw data from experimental spray measurement were analyzed and fitted using a software tool developed in the MATLAB programming environment. The obtained distribution characteristics were used as input in Ansys Fluent to set up appropriate injections. The spray was properly discretized and represented by a sufficiently large number of computational droplets. The spray simulation was finally validated by comparing the computed data with the experimental data.

It has been shown that Ansys Fluent is able to represent reasonably well sprays in terms of overall drop size distribution. However, in case one is interested in a more detailed spray description then more sophisticated atomizer models or complex injections may be necessary.

Acknowledgement

The authors gratefully acknowledge financial support of the Ministry of Education, Youth and Sports of the Czech Republic within the framework of project No. 2B08048 "Waste as raw material and energy source".

References

[1] Lefebvre, A.H., Wang, X., and Martin, C., *Journal of Propulsion and Power*, 4:293-298 (1988).
[2] Sovani, S.D., Sojka, P.E., and Lefebvre, A.H., *Progress in Energy and Combustion Science*, 27: 483-521 (2001).
[3] Ramamurthi,, U. Sarkar, K., and Raghunandan, B., *Atomization and Sprays*, 19:41-56 (2009).
[4] Jiang, X., Siamas, G., Jagus, K., and Karayiannis, T., *Progress in Energy and Combustion Science*, 36:131-167 (2010).
[5] Riber, E., Moureau, V., García, M., Poinsot, T., and Simonin, O., *Journal of Computational Physics*, 228:539-564 (2009).
[6] Jedelský, J., Jícha, M., and Sláma, J., *19th International Conference on Liquid Atomization and Spray Systems - ILASS Europe*, Nottingham, UK, 2004, pp. 521-526.
[7] Rosin, P., and Rammler, E., *J. Inst. Fuel*, 7:29–36 (1933).
[8] Calay, R., and Holdo, A., *Journal of Hazardous Materials*, 154:1198-1209 (2008).
[9] Cleary, V., Bowen, P., and Witlox, H., *Journal of Hazardous Materials*, 142:786-796 (2007).
[10] Ayres, D., Caldas, M., Semiao, V., and Carvalho, M.D.G., *Fuel*, 383-394 (2000).
[11] Babinsky, E., and Sojka, P.E., *Progress in Energy and Combustion Science*, 28:303-329 (2002).
[12] Shuai, S., Abani, N., Yoshikawa, T., Reitz, R.D., and Park, S.W., *Fuel*, 88:1235-1244 (2009).
[13] Shuai, S., Abani, N., Yoshikawa, T., Reitz, R.D., and Park, S.W., *International Journal of Thermal Sciences*, 48:1786-1799 (2009).
[14] Xiong, H., Lin, J., and Zhu, Z., *Atomization and Sprays*, 19:75-90 (2009).
[15] Lund, M., Sojka, P., Lefebvre, A.H., and Gosselin, P., *Atomization and Sprays*, 77-89 (1993).
[16] Qian, L., Lin, J., and Xiong, H., *Chinese Journal of Chemical Engineering*, 17:8-19 (2009).
[17] Jedelsky, J., Jicha, M., Slama, J., and Otahal, J., *Energy & Fuels*, (2009).
[18] Lagarias, J.C., Reeds, J.A., Wright, M.H., and Wright, P.E., *SIAM Journal on Optimization*, 9:112-147 (1998).
[19] *Ansys Fluent 12.1 Documentation*, 2009.
[20] Morsi, S.A., and Alexander, A.J., *Journal of Fluid Mechanics Digital Archive*, 55:193-208 (1972).
[21] Kermes, V. and Bělohradský, P., *Energy*, 33:1551-1561 (2008).